Environmental Science & Technology

Article

Cite This: Environ. Sci. Technol. 2018, 52, 3016−3026

pubs.acs.org/est

Transformations of Phosphorus Speciation during (Hydro)thermal Treatments of Animal Manures

Rixiang Huang,[†] Ci Fang,[†,‡] Bei Zhang,[†] and Yuanzhi Tang*[,†]

[†]School of Earth and Atmospheric Sciences, Georgia Institute of Technology, 311 Ferst Drive, Atlanta, Georgia 30324-0340, United States

[‡]College of Resources and Environmental Sciences, China Agricultural University, Beijing 100193, China

Supporting Information

ABSTRACT: Phosphorus (P) in animal manures is an important P pool for P recycling and reclamation. In recent years, thermochemical techniques have gained much interests for effective waste treatment and P recycling. This study comparatively characterized the transformation of P during two representative thermochemical treatments (pyrolysis and hydrothermal carbonization, HTC) of four animal manures (swine, chicken, beef, and dairy manures) by combining nuclear magnetic resonance spectroscopy, X-ray absorption spectroscopy, and sequential extraction. For both pyrolysis and HTC treatments, degradation of organic phosphate and crystallization of Ca phosphate minerals were observed and were highly dependent on treatment temperature. Extensive crystallization of Ca phosphate minerals occurred at temperatures above 450 °C during pyrolysis, compared to the lower temperature (175 and 225 °C) requirements during HTC. As a result, P was immobilized in the hydrochars and high temperature pyrochars, and was extracted primarily by HCl. Because Ca is the dominating P-complexing cation in all four manures, all manures showed similar P speciation and transformation behaviors during the treatments. Results from this work provided deeper insights into the thermochemical processes occurred during the pyrolysis and HTC treatments of biological wastes, as well as guidance for P reclamation and recycling from these wastes.

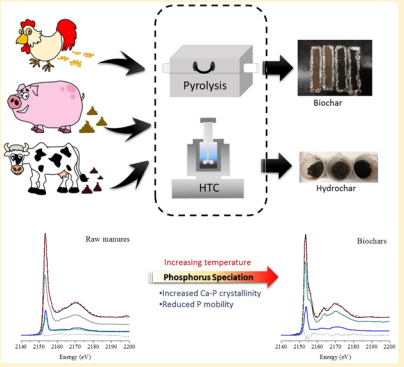

1. INTRODUCTION

Animal manures contain significant amount of nutrients such as nitrogen (N) and phosphorus (P) that are critical for crop growth. P in animals wastes (feeds from fertilized crops and nonfertilized rangeland) amounts to 7 million tons per year, equivalent to around 40% of total human mined P.[1] Soil application of animal manures is a common agriculture practice with a long history, serving as both a waste disposal option and a nutrient recycling practice. However, serious environmental issues are associated with this strategy if manures were not properly treated before their land applications. First, N and P embedded in manures are highly mobile and can become non-point-source contributors of eutrophication in various water bodies.[2,3] Second, manures typically contain a wide range of pathogens and organic contaminants (e.g., antibiotics) that can adversely impact human health and ecosystem upon their release into the environment.[4,5] Under the current socio-economic and environmental presses for sustainability, such as the concerns for P resource depletion, costs associated with N and P fertilizer production,[6] and contaminations due to manure soil application, it is highly desired to develop new strategies for manure management.

In recent years, (hydro)thermal techniques have emerged as promising treatment techniques for solid biowastes (e.g., sludges, manures, and food wastes), as they can simultaneously target resource recovery and environmental protection[7,8] by significantly reducing waste volume, degrading pathogens and organic contaminants,[9,10] and transforming biowastes into biofuels (gas, liquid, or solid chars), sorbents, or soil amendments.[11−15] Extensive studies have been devoted to characterize the overall properties of products from (hydro)-thermal treatments and the transformation of carbon (C), because C is the most abundant element in biomass and governs the properties and functionality of the products.[16−20] P is an abundant element in animal manures, ranging from 0.3 to 4.9 wt % (dry mass).[21] Considering the significance of manure P in P cycling and recycling, it is also important to characterize the transformation of P speciation and the effects of treatment conditions. Such information can provide guidance for the selection of treatment techniques and conditions for effective P recycling practice. For example, if the treatment products are to be used for soil fertilization, P content and speciation in the treatment products (e.g., solid chars) will determine their nutrient recycling efficiency and overall quality as fertilizers.[15,22−24]

Two representative (hydro)thermal treatment techniques are pyrolysis (dry thermochemical treatment) and hydrothermal

Received: October 10, 2017
Revised: December 23, 2017
Accepted: January 30, 2018
Published: February 12, 2018

DOI: 10.1021/acs.est.7b05203
Environ. Sci. Technol. 2018, 52, 3016−3026

Table 1. Treatment Conditions and Sample Labels

feedstock	pyrolysis				ashing	HTC	
	250 °C	350 °C	450 °C	600 °C	550 °C	175 °C	225 °C
swine manure	Sw250	Sw350	Sw450	Sw600	Sw_Ash	SwHTC175	SwHTC225
chicken manure	Ch250	Ch350	Ch450	Ch600	Ch_Ash	ChHTC175	ChHTC225
beef manure	Bf250	Bf350	Bf450	Bf600	Bf_Ash	BfHTC175	BfHTC225
dairy manure	D250	D350	D450	D600	D_Ash	DHTC175	DHTC225

carbonization (HTC, wet thermochemical treatment), both operating at low to medium temperature range and with relatively high mass recovery in the solid products (pyrochars for pyrolysis, hydrochars for HTC). Previous studies have examined the transformation of P during pyrolysis of plants and manures, such as the changes in P molecular moiety by combined chemical extraction and ^{31}P liquid nuclear magnetic resonance (NMR) analysis.[25−27] A few studies also investigated the behavior of P during hydrothermal treatments of manures, but the focus was primarily on the distribution of P between solid and liquid phases as a function of treatment conditions.[28−31] An in-depth understanding of the thermochemical mechanisms behind P transformation during these treatment processes is still missing. The complexation and mineralogy states of P in the solid products were also less explored, despite their significance in controlling the mobility and availability of P.

We recently studied the speciation transformation of P (molecular moiety, complexation, and mineralogy) during pyrolysis and HTC treatments of sewage sludges.[32,33] This study systematically investigates the speciation transformation of P during pyrolysis and HTC treatments of four different types of manures (swine, beef cattle, dairy cattle, and chicken manures). Since sewage sludges and animal manures are significantly different in their chemical composition and P speciation,[34] this study serves as a further exploration on the effects of feedstock composition on P speciation and transformation. Combined ^{31}P NMR, synchrotron X-ray absorption spectroscopy (XAS), and sequential chemical extraction analysis were used to thoroughly characterized P speciation and mobility in the raw and treated manures. Findings from this work can help gain a better understanding of the thermochemical reactions during pyrolysis and HTC treatment of solid biowastes, as well as the effects of feedstock properties and treatment conditions on P speciation and mobility in the final solids.

2. EXPERIMENTAL APPROACH

2.1. Sample Collection. Animal manures were collected from local farms in the vicinity of Atlanta, GA, USA. Swine and beef cattle manures were collected from a farm where the pigs were mainly fed with grains and the beef cattle with grain, hay, and grass. Dairy cattle manure and chicken manure were collected from farms where the dairy cattle were fed with grass and chickens with grains. Lime was occasionally spread on the ground of the henhouse. Upon sample collection, the moist manures were immediately stored at −20 °C. A portion of each feedstock was also freeze-dried for pyrolysis and elemental analysis.

2.2. Pyrolysis and HTC Treatment. Pyrolysis of the freeze-dried samples was carried out using a tube furnace (Thermo Scientific) under argon flow (∼1 mL/sec) at a range of holding temperatures (250−600 °C), with a heating and cooling rate of 200 °C/h and a soaking duration of 4 h. For each treatment condition, 1.0 g of freeze-dried manure was added into a crucible and inserted into the glass tube. All samples were processed in duplicate. The produced solid chars are referred to as pyrochar. A portion of the freeze-dried samples was also ashed at 550 °C for 4 h in air, and characterized and compared with the pyrolysis samples.

For HTC treatments, wet manures equivalent to ∼2.0 g dry mass were weighed into a 20 mL Teflon-lined stainless steel hydrothermal reactor (Parr instrument). Deionized water (DI) was then added to achieve a total weight of 12 g (equivalent to solid/liquid ratio of 1:5). The reactors were sealed and heated in an oven at 175 or 225 °C for 4 h and then allowed to naturally cool down to 50 °C in the oven. The produced solids (hereafter referred to as hydrochars) and processed water were separated by centrifugation, and the hydrochars were freeze-dried for further analysis. Treatment conditions and sample labels are summarized in Table 1.

2.3. Sequential Extraction. Sequential extraction of the raw manures and their derived hydrochars was conducted following the Hedley's method.[35] The extraction method considers the P species extracted by water, $NaHCO_3$, NaOH, and HCl to be readily soluble P, exchangeable P, Fe/Al mineral adsorbed P, and insoluble phosphates, respectively. Specifically, 100 mg of raw manure or char was added to a 50 mL polypropylene centrifuge tube and sequentially extracted by 20 mL extraction solutions, including deionized water (DI), 0.5 M $NaHCO_3$, 0.1 M NaOH, and 1.0 M HCl solutions, each lasting 16 h. The sample tubes were constantly agitated by end-to-end shaking. All experiments were conducted in replicate. At the end of each extraction step, the solid and aqueous phases were separated by vacuum filtration (0.45 μm). The filtrate was digested using the persulfate digestion method (APHA, 2012)[36] and analyzed for P concentration using the phosphomolybdate colorimetric assay[37] on an UV−vis spectrometer (Carey 60, Agilent). Note that variability can exist in P concentration determined in sequential extracts using colorimetric method, especially for samples with low P concentrations.[38] The residual solids at the end of sequential extraction were freeze-dried, combusted at 600 °C in a furnace for 4 h, extracted by 4 M HCl for 16 h, and analyzed for P concentration using the method described above.

2.4. X-ray Powder Diffraction Analysis. X-ray diffractograms (Cu Kα radiation) of raw manures and reference Ca phosphate minerals were collected using a PANalytical Empyrean X-ray diffractometer at 15−60° 2θ, with a step size and dwell time of 0.013° and 50 ms, respectively.

2.5. Liquid ^{31}P NMR Spectroscopy. A portion of the freeze-dried manures and their chars were extracted using a solution containing 0.25 M NaOH and 0.05 M EDTA at a solid:liquid ratio of 0.2:4 g/mL and was shaken at 150 rpm for 16 h at room temperature. At the end of extraction, liquid extracts and solid residues were separated by centrifugation. 600 μL of the supernatant was mixed with 100 μL of D_2O for liquid ^{31}P NMR measurements. NMR spectra of the liquid

DOI: 10.1021/acs.est.7b05203
Environ. Sci. Technol. 2018, 52, 3016−3026

samples were obtained using a Bruker AMX 400 MHz spectrometer operated at 162 MHz at 297 K. Parameters of 90° pulse width, 6.5K data points (TD) over an acquisition time of 0.51 s, and relaxation delay of 15 s were applied.

2.6. P K-Edge X-ray Absorption Near-Edge Structure (XANES) Spectroscopy Analysis. P K-edge XANES is the main technique capable of characterizing in situ P speciation in complex matrices such as solid wastes.[34] P XANES data were collected at Beamline 14-3 at the Stanford Synchrotron Radiation Lightsource (SSRL), Menlo Park, CA. Dried solids of the raw manures and their chars were ground into fine powders and brushed evenly onto P-free Kapton tapes, and the sample-loaded tapes were mounted to a sample holder. P XANES spectra were collected in fluorescence mode using a PIPS detector, during which the sample chamber was kept under helium atmosphere at room temperature. Energy calibration used $AlPO_4$ (edge position 2152.8 eV). Spectra of $AlPO_4$ were periodically collected to monitor possible energy shifts, which was not observed during the entire data collection period. XANES spectra were collected at 2100−2485 eV. Two scans were collected for each sample and averaged for further analysis.

Data processing and analysis were performed using the software Ifeffit.[39] All spectra were carefully examined for energy calibration, merged, and normalized. Linear combination fitting (LCF) was conducted on the XANES spectra at an energy range of −15 to +50 eV. E_0 values of reference compounds were allowed to float up to ±1 eV. The sample spectra were analyzed using principal component analysis (PCA) to determine the number of principle components needed to reconstruct sample spectra. Target transformation was used to select the appropriate reference compounds for subsequent linear combination fitting. The goodness of fit was evaluated using the residual factor (*R* factor), and the fit with smallest *R* factor was deemed best fit. Because Ca, Mg, Al, and Fe are the main phosphate-complexing cations in manures, a spectral library of their corresponding phosphate compounds were used for LCF analysis, including phytic acid (representating organic phosphates), $AlPO_4$, $FePO_4{\cdot}2H_2O$, struviate ($NH_4MgPO_4{\cdot}6H_2O$), $CaHPO_4$, $Ca(H_2PO_4)_2$, amorphous Ca phosphate (ACP), 10% Mg-doped ACP (ACP10Mg), ACP treated at 600 °C (ACP600C), and hydroxylapatite (HAP). Details of these reference compounds can be found in the Table S1, and their P K-edge XANES spectra are shown in Figure S1. Mineralogy of the synthetic Ca−phosphate phases (ACP, ACP10Mg, ACP600C, and HAP) was confirmed by X-ray diffraction (Figure S2). The reason for including both pure and Mg-doped ACP in LCF analysis was because Mg is the second most abundant cation (after Ca) in all manure samples (Table 2) and has been previously shown to readily incorporate into Ca phosphate minerals.[40,41] The difference between these two phases is mainly in the white line intensity. The detailed LCF results can be found in Table S2.

3. RESULTS AND DISCUSSION

3.1. Overall Chemical Characteristics of the Raw Animal Manures. Concentrations of the major elements (C, N, P, Ca, Mg, Fe, and Al) in the raw manure samples are present in Table 2. In general, swine and chicken manures have higher P contents (both ~2%) than beef and dairy manures (0.89 and 0.58%, respectively). Ca is the most dominant cation in all manures, with concentrations ranging from 14.8 g/kg (dairy manure) to 52.8 g/kg (chicken manure). Mg is the

Table 2. Major Element Contents in the Raw Manure Samples

		elemental content							metal/P molar ratio			
feedstock	ash content (%)	C (%)	N (%)	P (%)	Ca (g/kg)	Mg (g/kg)	Fe (g/kg)	Al (g/kg)	Ca/P	Mg/P	Fe/P	Al/P
swine manure	14.2	41.88 ± 1.72	4.52 ± 0.28	1.97 ± 0.28	24.50 ± 6.37	7.94 ± 0.22	0.87 ± 0.02	1.46 ± 0.16	0.96	0.52	0.02	0.09
chicken manure	46.8	27.54 ± 2.02	2.96 ± 0.15	1.69 ± 0.30	52.83 ± 6.10	6.03 ± 0.06	5.06 ± 0.75	4.89 ± 0.25	2.42	0.46	0.17	0.33
beef manure	12.6	40.90 ± 1.15	3.14 ± 0.27	0.89 ± 0.14	23.29 ± 3.31	9.62 ± 1.04	1.51 ± 0.20	1.58 ± 0.26	2.02	1.39	0.10	0.20
dairy manure	10.9	46.32 ± 2.37	2.42 ± 0.01	0.58 ± 0.14	14.83 ± 1.12	7.89 ± 0.62	0.28 ± 0.02	0.25 ± 0.01	1.98	1.75	0.03	0.05

DOI: 10.1021/acs.est.7b05203
Environ. Sci. Technol. 2018, 52, 3016−3026

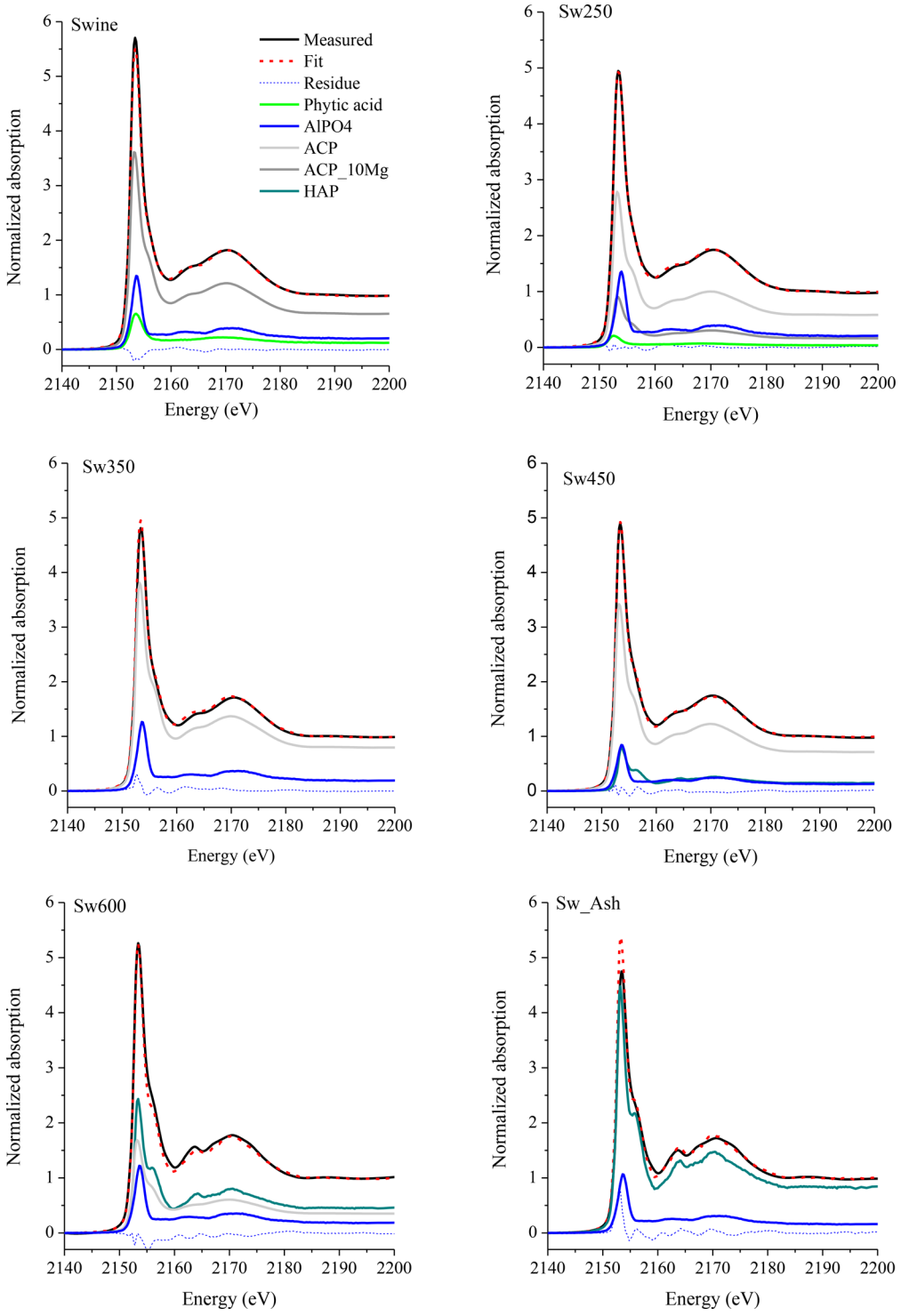

Figure 1. LCF of P K-edge XANES spectra of swine manure and its pyrochars (250−600 °C) and ash. LCF analysis of other manures can be found in the Supporting Information.

second abundant metal, with concentrations ranging from 6 to 10 g/kg. Chicken, beef, and dairy manures contain similar concentrations of Fe and Al, at ~5 g/kg for chicken manure, ~1.5 g/kg for beef manure, and ~0.25 g/kg for dairy manure. Swine manure contains slightly more Al (1.46 g/kg) than Fe (0.87 g/kg). The molar ratio of Ca and Mg to P is close to or larger than 1, while the ratio of Al and Fe to P ranges from 0.03 to 0.33 (Table 2). The molar ratios suggest that P may be primarily complexed by Ca, since pure Mg phosphates are generally soluble and Al and Fe can present as other minerals phases (reducing their capacity to complex P). No crystalline minerals were observable in the raw manures, except for chicken and beef manures (both containing quartz and calcite) (Figure S3).

P speciation in the raw manure was probed by ^{31}P NMR and P XANES spectroscopy. ^{31}P liquid NMR analysis of the liquid extracts from manures showed the predominant presence of orthophosphate and a small fraction of organic phosphates

DOI: 10.1021/acs.est.7b05203
Environ. Sci. Technol. 2018, 52, 3016−3026

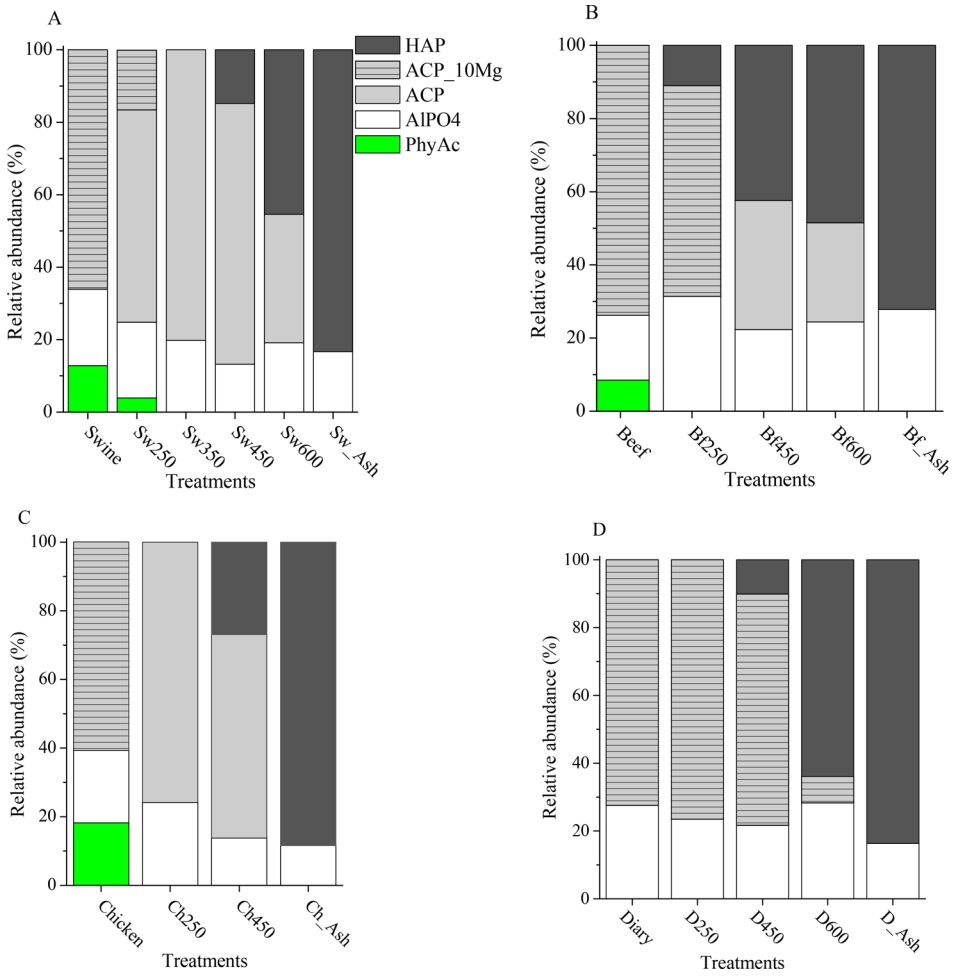

Figure 2. Relative abundance of different P species in swine manure and its pyrochars (A), beef manure and its pyrochars (B), chicken manure and its pyrochars (C), and dairy manure and its pyrochars (D), as quantified by LCF of the P XANES spectra (Figure 1).

(Figure S4). However, solution extraction only extracts readily soluble or desorbed P fractions and cannot provide information on the complexation and mineral states of P. Therefore, P K-edge XANES was used to probe the in situ speciation of P in the raw feedstocks.

P XANES spectra of the raw manures display three distinctive features that are indicative of calcium phosphate phases: a postedge shoulder at ~2156 eV, the first peak at ~2164 eV, and a second peak at ~2172 eV (Figure 1 and Figures S1 and S5). This suggests the presence of abundant calcium phosphate phase(s) in all samples. LCF results confirmed that the dominant P species in the raw manures is amorphous Ca phosphate, with relative abundance ranging from 60 to 72% (Figure 2). The other P species are Al phosphate phase(s) (fitted as $AlPO_4$) and organic phosphates (fitted as phytic acid). The dominance of Ca phosphate phases is consistent with elemental composition results that Ca is the most abundant cation (with highest metal/P ratio) for P complexation (Table 2). Phytic acid is ubiquitous in all kinds of animal manures (usually the predominant organic phosphate species), since common feeds for animals (e.g., grass, hay, and grains) consist of abundant phytic acid.[42,43]

These results are consistent with previous studies on P speciation in animal manures, which has been extensively studied using sequential extraction, ^{31}P liquid/solid state NMR, and/or P K-edge XANES. Although P speciation is generally found to be affected by animal type, diet, growth stage, and postprocessing method, the dominant P species are typically Ca phosphates, organic phosphates, and Al/Fe-associated phosphate species.[43−45]

3.2. Effects of Pyrolysis on P Speciation. The phase migration behavior of P during pyrolysis of various biowastes (including manures) has been extensively studied and P was found to mostly remain in the solid phase at low to mid temperature range.[34,46,47] P XANES spectra of pyrochars from all manures exhibit a similar temperature-dependent change, with the distinctive spectral features of Ca phosphates (peaks at ~2164 and ~2172 eV) becoming more prominent at elevated heating temperatures (Figure 1 and Figure S5). LCF analysis of the P XANES spectra suggests the following changes (Figure 2): (1) Organic phosphate species (fitted as phytic acid) was degraded by pyrolysis. For swine manure, phytic acid was only detected at <5% (of total P) after 250 °C treatment, and completely disappeared after treatment at higher temperatures. For beef, chicken, and dairy manures, no phytic acid was identified at temperature above 250 °C. (2) For all manure types, the relative abundance of Ca phosphate species generally increased with increasing pyrolysis temperature. (3) Amorphous Ca phosphates gradually transformed into crystalline Ca phosphate phase (fitted as hydroxylapatite), and the crystallinity increased with increasing pyrolysis temperature. (4) Ashing at 550 °C (4 h) resulted in more crystallization than

DOI: 10.1021/acs.est.7b05203
Environ. Sci. Technol. 2018, 52, 3016−3026

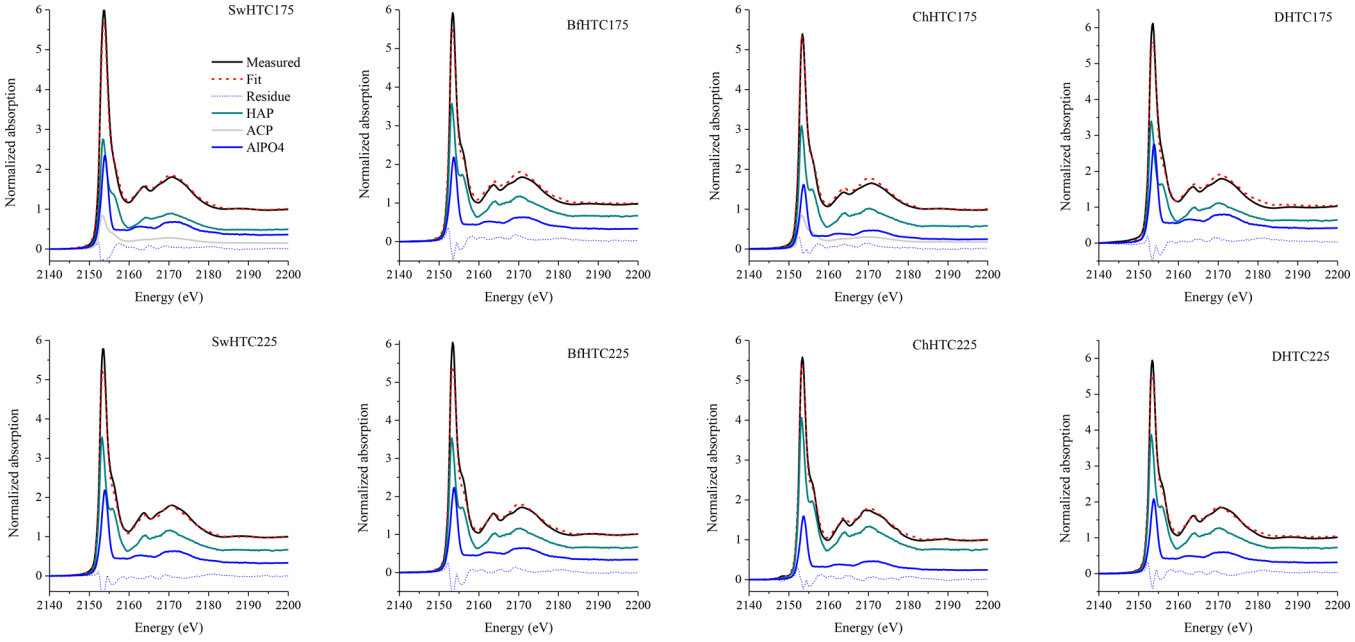

Figure 3. LCF results of P XANES spectra of swine, beef, chicken, and dairy hydrochars produced at 175 (upper panels) and 225 °C (lower panels).

pyrolysis at similar heating intensity (600 °C, 4 h). The reaction mechanisms behind these transformations are discussed in Section 3.5.

3.3. Effects of HTC on P Speciation. Mass recovery in the solid hydrochars ranged from ~54 to ~74%, depending on feedstock and treatment temperature (Table S3). In general, mass recovery in the solid phase decreased with increasing temperature because of enhanced volatilization/solubilization of organic matters into the gaseous/liquid phases. P recovery in the hydrochars ranged from ~73 to ~100%, with the recovery of chicken manure being the highest and swine manure the lowest, because chicken manure has a higher Ca/P ratio. The recovery of P in solid products depends on a range of factors, including feedstock types and treatment conditions (temperature, duration, and solution chemistry).[28,29,48] Elemental composition (particularly phosphate precipitating metals such as Ca, Al, and Fe) may be the most important factor, because it determines the potential of phosphate retainment in the solid phase.

Similar to pyrolysis treatment, P XANES spectra of hydrochars all showed increasing sharpness of the distinctive spectral features of Ca phosphates (postedge shoulder at ~2156 eV, peaks at ~2164 and ~2172 eV), regardless of manure types (Figure 3). LCF analysis of the P XANES spectra also revealed the decrease (decomposition) of organic phosphates (fitted as phytic acid), the decrease of amorphous Ca-phosphate phases, and the increase of crystalline Ca phosphate phase (fitted as hydroxylapatite) (Figure 4A). Liquid ^{31}P NMR also confirmed the disappearance of organic phosphates in the liquid extracts of 225 °C hydrochars (Figure S4). Almost all Ca phosphate phases were converted to crystalline hydroxylapatite phase at 225 °C (Figure 4A). Overall, the abundance of $AlPO_4$ species remained constant during HTC. Thermochemical mechanisms responsible for the transformation are discussed in section 3.5.

3.4. Sequential Extraction of P and Its Correlation to Chemical Speciation. Sequential extraction was used to evaluate the mobility of P in the manure samples after pyrolysis and HTC treatments, and to correlate with the P speciation information obtained by LCF analysis of XAS data. As previously mentioned, the Hedley extraction method considers the P species extracted by H_2O, $NaHCO_3$, NaOH, and HCl to be readily soluble P, exchangeable P, Fe/Al mineral adsorbed P, and insoluble phosphates, respectively.

For raw manures, sequential extraction results showed that P in all the raw manures was highly mobile (Figure 4B and Table S3). Dairy manure samples were not analyzed, considering their similar nature and chemical composition as beef manure samples. For both swine and beef manures, ~60% P can be extracted by H_2O and $NaHCO_3$. Because chicken manure was relatively dry and with the largest Ca/P ratio, its P was relatively immobile, with only ~32% in H_2O and $NaHCO_3$ fractions. The fact that abundant P in raw manures was highly mobile (extractable by H_2O and $NaHCO_3$) can be attributed to the presence of relatively soluble P species commonly present in fresh manures, such as various organic phosphates, soluble phosphates (such as Na and K phosphates), and soluble Ca phosphate species.[49,50] This is consistent with the presence of phytic acid and dominance of amorphous Ca phosphate in raw manures revealed by P XANES. For all manures, the NaOH-extractable fraction was small (<10%), suggesting the low abundance of Al/Fe mineral adsorbed P species. This is consistent with P XAS LCF results, which did not identify any mineral-adsorbed P species. The HCl fraction of swine and beef manures was small (19 and 5%, respectively), contributed by insoluble Al and Ca phosphate phases. This corresponds well with the presence of $AlPO_4$ and absence of crystalline Ca phosphate phases as suggested by LCF of P XAS.

Pyrolysis treatment of the swine manures overall immobilized P, and the effect was enhanced with increasing temperatures (Figure 4B and Table S3). At low pyrolysis temperature (250 °C), the main change was the decrease of the H_2O-extractable fraction (from 43% in raw swine to 25% in 250 °C sample) and increase of $NaHCO_3$ extractable fraction (from 14% in raw swine to 32% in 250 °C sample). At higher temperatures (350 to 600 °C), the H_2O extractable fractions were negligible (<5%) and the $NaHCO_3$ fraction stayed at

DOI: 10.1021/acs.est.7b05203
Environ. Sci. Technol. 2018, 52, 3016−3026

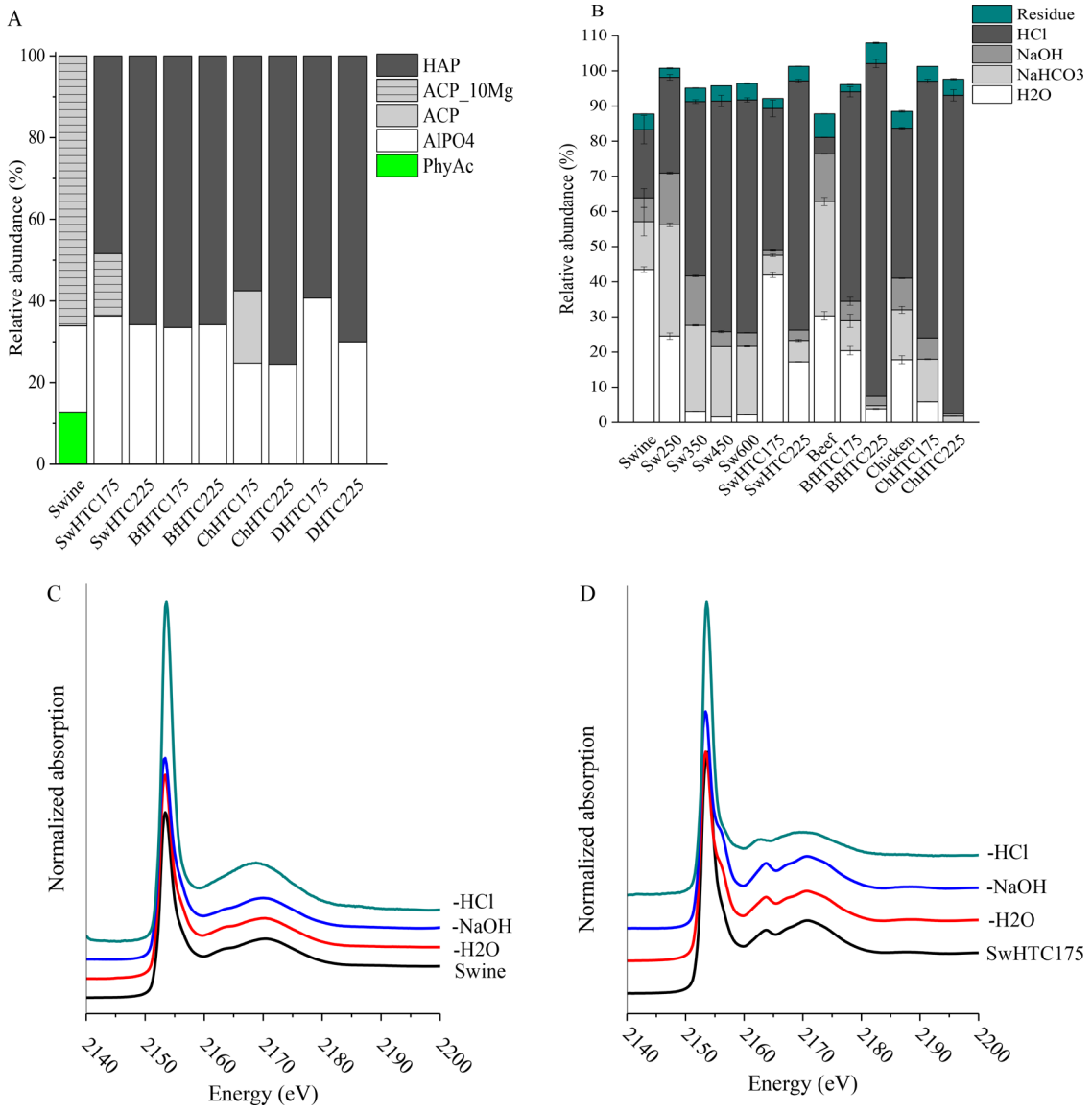

Figure 4. (A) Relative abundance of different P species in animal manures and their hydrochars, quantified by LCF of the P XANES spectra (data for raw manures other than swine were shown in Figure 2). (B) Relative abundance of P (percentage of total P) in sequential extraction solution for raw manures and their chars (raw data expressed as mass concentration can be found in Table S3). Error bars represents standard deviation of replicate experiments. (C, D) Normalized P XANES spectra of solid residues after sequential extractions for raw swine manure and its HTC175 hydrochar, respectively.

~20−25%. Overall, the HCl extractable fractions gradually increased with increasing treatment temperature, from ~20% (raw manure) to ~66% (600 °C sample). These results are consistent with the gradual crystallization of Ca phosphates and degradation of organic phosphate with increasing pyrolysis temperatures, as revealed by P XANES analysis (Figures 1 and 2).

After HTC treatment, P fractionation for all manure samples experienced similar changes, including the gradual decrease of H_2O- and $NaHCO_3$-extractable fractions and increase of the HCl-extractable fraction with increasing treatment temperature (Figure 4B). Compared to raw swine and beef manures (both with only ~20% P in the HCl fraction), their hydrochars contain 40−80% P in the HCl fraction, and the relative abundance increased with increasing temperature. For chicken manure, the HCl fraction increased from 42% (raw manure) to 73% and 91% for its 175 and 225 °C hydrochars, respectively. The increased P proportion in the HCl fraction after HTC treatment is consistent with the transformation of amorphous Ca phosphate phases into the less soluble crystalline Ca phosphate phase, as revealed by P XANES analysis (Figure 4A).

As discussed above, in general the P species identified by sequential extraction and XAS can qualitatively correlate with each other. However, caution should be taken to quantitatively correlate these results, especially for raw manures (Figure 4A and 4B). For example, for swine and beef manures, ~40, 20, and 20% of total P were present as H_2O-, $NaHCO_3$-, and HCl-extractable fractions, respectively, while ~10, 20, and 70% of the total P were identified by XAS as phytic acid, $AlPO_4$, and amorphous Ca phosphate. To further probe the possible P species being extracted during sequential extraction, solid residues after sequential extraction steps (with substantial P removal) were also characterized with P XANES analysis. For raw swine manures, no substantial spectral changes were

DOI: 10.1021/acs.est.7b05203
Environ. Sci. Technol. 2018, 52, 3016−3026

observed after H_2O, $NaHCO_3$, and NaOH extractions (despite >60% P removal), and LCF analysis indicated only the decrease of phytic acid (Figure 4C and Table S2). Considering the relative abundance of phytic acid and the percent of P removal, it is likely that phytic acid were preferentially removed and P species in the spectrally-identified forms of $AlPO_4$ and ACP were also substantially removed during H_2O, $NaHCO_3$, and NaOH extractions. In comparison, the relative percentage of phytic acid increased while that of amorphous Ca phosphate decreased after H_2O, $NaHCO_3$, and NaOH extractions of beef manure, possibly due to more removal of amorphous Ca phosphate than phytic acid (e.g., undigested hay and grass in beef manure). After HCl extraction, the spectral features of amorphous Ca phosphate disappeared for both swine and beef manures, supporting the primary removal of Ca phosphate phases during HCl extraction (Figure 4C and Figure S6). For 175 °C hydrochars of swine and beef manures, the spectral features of hydroxylapatite (shoulder at 2156 eV, peaks at ~2164 and ~2172 eV) persisted after H_2O, $NaHCO_3$, and NaOH extractions, and disappeared after HCl extraction (Figure 4D and Figure S6). Correspondingly, LCF analysis showed the removal of crystalline Ca phosphate only during the HCl extraction step (Table S2). The discrepancy between sequential extraction and XAS results in terms of species/fraction abundance suggests that, some species (e.g., those soluble in H_2O, $NaHCO_3$, and NaOH extraction solutions) were not identified by XAS, possibly due to the limited numbers of reference compounds used. For example, the P species identified by XAS to be amorphous Ca phosphates and $AlPO_4$ phases may possibly include some soluble or mineral-adsorbed species, such as Na/K phosphate salts or phosphate adsorbed on Al-minerals, because their spectra contain less distinct features as compared to the (crystalline) Ca phosphate phases.[51,52]

As we have discussed previously,[33,34] such discrepancy between chemical extraction and XAS fitting results is likely due to the intrinsic limitations of both methods: (1) P pools from sequential extraction are operationally defined and the exact P species extracted in each solution are only loosely categorized.[53] In addition, P speciation can be altered during the extraction process. (2) Not all P species in complex samples such as animal manures can be identified by LCF analysis of P XANES spectra, because only a limited number of reference compounds can be included. (3) Compounds with less distinctive spectral features may not be identified and/or accurately quantified (such as different organic phosphates sharing similar spectral features[52,54]), because LCF analysis is a mathematical method based on spectral features.

3.5. P Transformation Mechanisms. Results from this study revealed the similarities and differences between pyrolysis and HTC treatments of animal manures, regarding their effects on the transformation of P speciation. Pyrolysis is a dry thermochemical process, during which nonvolatile elements such as P and metals may not be able to freely migrate or interact with each other. In contrast, HTC is a wet thermochemical process with reactions occurring in aqueous phase,[55] thus, the reaction environment is relatively homogeneous and elements have higher freedom to interact with each other.

Both treatments shared a similar trend that organic phosphates were decomposed even at low treatment temperatures. However, the transformation pathways and the thermochemical reactions involved are likely different. Previous studies using chemical extraction and liquid ^{31}P NMR analysis revealed that pyrolysis can transform organic phosphates into orthophosphate (via degradation of the linked organic groups), pyrophosphate (via dehydration), or more stable organic phosphates (polymerization of the organic groups, which can not be extracted and characterized by liquid ^{31}P NMR).[25,27,33] In comparison, organic phosphates are most likely degraded via hydrolysis during HTC treatment, and the released orthophosphate may undergo precipitation or adsorption to form other inorganic phosphate species.[32,33]

The transformation of inorganic phosphates during pyrolysis is temperature dependent. This study demonstrated that observable transformation was only found at high temperature range, consistent with a previous study on the pyrolysis of anaerobic digestate (75% pig/dairy slurry and 25% food wastes), which showed significant formation of hydroxylapatite only at pyrolysis temperatures above 600 °C.[56] In addition to temperature, heat-driven crystallization of Ca phosphate phases can also be affected by matrix composition. For example, during the pyrolysis of slaughterhouse wastes (consist of mostly bones), increasing amounts of hydroxylapatite formed from amorphous Ca phosphate as the pyrolysis temperature increased from 220 to 750 °C, while such a trend was less evident in the presence of plant biomass.[57] In addition to Ca phosphate crystallization, replacement of the cations in other inorganic phosphates by Ca is also possible. For example, a previous study found the transformation of Al and Fe phosphates into apatite during the incineration of sewage sludge.[58]

The increasing abundance of Ca phosphates with increasing crystallinity and enhanced P immobilization after HTC treatment suggest that (1) orthophosphate was released from organic phosphate and complexed by Ca and (2) initial soluble P species (e.g., Na/K phosphates) may also be dissolved and form more stable and less soluble phases during HTC. Since Ca is the most abundant cation in manures and has high affinity to phosphate, the increasing abundance of Ca phosphate phases after HTC treatment is not surprising. The formation of crystalline Ca phosphates under hydrothermal conditions is also well established and relevant to many environmental and geological processes, and can occur through several different pathways. For example, studies have showed the displacement of Ca carbonate phase with apatite during the diagenesis process,[59] as well as the formation of hydroxylapatite from $Ca(OH)_2$ and $CaHPO_4{\cdot}2H_2O$ under hydrothermal conditions.[60] These studies suggest that hydroxylapatite is the stable Ca phosphate phase under hydrothermal conditions, which is consistent with our LCF results showing the dominant presence of hydroxylapatite after HTC treatments, regardless of feedstock. However, the degree of dissolution, reprecipitation, and/or crystallization of Ca phosphates can be affected by HTC temperature. For example, in this study, the crystallization at 175 °C is not as complete as that at a higher treatment temperature (225 °C) (Figure 4A).

Results from this study and previous studies also suggest that metal stoichiometry and affinity to P largely determine the P speciation evolution during HTC treatment. Our previous study on sewage sludge showed that the P was increasingly associated with Fe (as sorbed P species on Fe oxides) and Ca (as Ca phosphate phases), since both Ca and Fe are abundant in sludges.[33] As also shown in this work, adding dissolved $FeCl_3$ into manures during HTC treatment can substantially modify P speciation in the hydrochars (Figure S7). Such finding might be

DOI: 10.1021/acs.est.7b05203
Environ. Sci. Technol. 2018, 52, 3016−3026

generalized to the treatment of other biowastes, where different metal cations might be present at varied concentrations.

4. ENVIRONMENTAL IMPLICATIONS

A mechanistic understanding of the transformation of critical elements in solid biowastes is fundamental for the optimization of treatment techniques for different purposes. This study quantitatively characterized the transformations of P during pyrolysis and HTC treatments (representative of dry and wet thermochemical treatments, respectively) of different animal manures, and explored the effects of treatment temperature and feedstock characteristics on P speciation and mobility in the treatment products. In general, degradation of organic phosphates and increase of Ca-phosphate minerals (as well as their crystallinity) were found to occur with increasing treatment temperature, which correlates well with the overall reduction of P mobility in the treated solids. Combined with our previous studies on P speciation transformation in sewage sludges during (hydro)thermal treatments,[32−34] it is reasonable to anticipate overall increased association of P with different metal cations (e.g., Ca, Fe, Al) and increased crystallinity of the phosphate mineral phases, which can lead to the overall reduced mobilization of P in the treated solids. Composition of the feedstock, such as concentrations of the dominant metal cations, can also provide insights on the dominant metal phosphate species (and related P mobility) in the treated products. In this regard, P speciation in different biowastes might also be tuned by adjusting treatment technique and conditions according to feedstock matrix properties.

The fertilization potential of thermochemical treatment products depends on a variety of factors, such as nutrient speciation in the treatment products, properties of soil and treatment products, plant type and growth stage, local weather, and microbial activity. Among these factors, P speciation plays a key role in P mobility, bioavailability, and overall recyclability. Therefore, thermochemical treatments will enable the production of fertilizers with improved P efficiency (compared to raw manures and inorganic fertilizers) via P speciation modulation during the treatments, in addition to other waste management benefits such as decontamination and volume reduction. In addition to P speciation, future studies are needed to correlate elemental speciation and matrix properties of the treatment products with their performance as fertilizers and/or soil amendments, in order to effectively synchronize the biowaste management and agricultural practice systems for efficient nutrient (re)cycling.

■ ASSOCIATED CONTENT

Supporting Information

The Supporting Information is available free of charge on the ACS Publications website at DOI: 10.1021/acs.est.7b05203.

Normalized P K-edge XANES spectra of reference compounds; XRD patterns of pure Ca phosphate minerals; LCF of P XANES spectra of representative samples for beef, chicken, and dairy manures; solid phase mass and P recovery; liquid ^{31}P NMR data for extracts of raw manures and their hydrochars (PDF)

■ AUTHOR INFORMATION

Corresponding Author

*E-mail: yuanzhi.tang@eas.gatech.edu. Tel: 404-894-3814.

ORCID

Yuanzhi Tang: 0000-0002-7741-8646

Notes

The authors declare no competing financial interest.

■ ACKNOWLEDGMENTS

This work is supported by National Science Foundation Grant Nos. 1559087, 1605692, and 1739884. We thank Drs. Ellery Ingall and Amelia Longo (Georgia Tech) for help with C and N content analysis and beamline scientist Dr. Matthew Latimer at SSRL Beamline 14-3 for help with experimental setup. Portions of this research were conducted at the Stanford Synchrotron Radiation Lightsource (SSRL). Use of the Stanford Synchrotron Radiation Lightsource, SLAC National Accelerator Laboratory, is supported by the U.S. Department of Energy, Office of Science, Office of Basic Energy Sciences under Contract No. DE-AC02-76SF00515. This work was performed in part at the Georgia Tech Institute for Electronics and Nanotechnology, a member of the National Nanotechnology Coordinated Infrastructure, which is supported by the National Science Foundation (Grant ECCS-1542174).

■ REFERENCES

(1) Cordell, D.; Drangert, J.-O.; White, S. The story of phosphorus: Global food security and food for thought. *Global Environmental Change* **2009**, *19* (2), 292−305.

(2) Sharpley, A. N.; McDowell, R. W.; Kleinman, P. J. A. Phosphorus loss from land to water: integrating agricultural and environmental management. *Plant Soil* **2001**, *237* (2), 287−307.

(3) Withers, P. J.; Clay, S. D.; Breeze, V. G. Phosphorus transfer in runoff following application of fertilizer, manure, and sewage sludge. *J. Environ. Qual.* **2001**, *30* (1), 180−188.

(4) Venglovsky, J.; Sasakova, N.; Placha, I. Pathogens and antibiotic residues in animal manures and hygienic and ecological risks related to subsequent land application. *Bioresour. Technol.* **2009**, *100* (22), 5386−5391.

(5) Heuer, H.; Schmitt, H.; Smalla, K. Antibiotic resistance gene spread due to manure application on agricultural fields. *Curr. Opin. Microbiol.* **2011**, *14* (3), 236−243.

(6) Withers, P. J. A.; Elser, J. J.; Hilton, J.; Ohtake, H.; Schipper, W. J.; van Dijk, K. C. Greening the global phosphorus cycle: how green chemistry can help achieve planetary P sustainability. *Green Chem.* **2015**, *17* (4), 2087−2099.

(7) Pham, T. P. T.; Kaushik, R.; Parshetti, G. K.; Mahmood, R.; Balasubramanian, R. Food waste-to-energy conversion technologies: Current status and future directions. *Waste Manage.* **2015**, *38*, 399−408.

(8) Titirici, M.-M.; White, R. J.; Falco, C.; Sevilla, M. Black perspectives for a green future: hydrothermal carbons for environment protection and energy storage. *Energy Environ. Sci.* **2012**, *5* (5), 6796−6822.

(9) vom Eyser, C.; Palmu, K.; Schmidt, T. C.; Tuerk, J. Pharmaceutical load in sewage sludge and biochar produced by hydrothermal carbonization. *Sci. Total Environ.* **2015**, *537*, 180−186.

(10) vom Eyser, C.; Palmu, K.; Otterpohl, R.; Schmidt, T. C.; Tuerk, J. Determination of pharmaceuticals in sewage sludge and biochar from hydrothermal carbonization using different quantification approaches and matrix effect studies. *Anal. Bioanal. Chem.* **2015**, *407* (3), 821−830.

(11) Parshetti, G. K.; Liu, Z. G.; Jain, A.; Srinivasan, M. P.; Balasubramanian, R. Hydrothermal carbonization of sewage sludge for energy production with coal. *Fuel* **2013**, *111*, 201−210.

(12) He, C.; Wang, K.; Yang, Y. H.; Wang, J. Y. Utilization of Sewage-Sludge-Derived Hydrochars toward Efficient Cocombustion with Different-Rank Coals: Effects of Subcritical Water Conversion and Blending Scenarios. *Energy Fuels* **2014**, *28* (9), 6140−6150.

(13) Weber, B.; Stadlbauer, E. A.; Schlich, E.; Eichenauer, S.; Kern, J.; Steffens, D. Phosphorus bioavailability of biochars produced by thermo-chemical conversion. *J. Plant Nutr. Soil Sci.* **2014**, *177* (1), 84−90.
(14) Liang, Y.; Cao, X. D.; Zhao, L.; Xu, X. Y.; Harris, W. Phosphorus Release from Dairy Manure, the Manure-Derived Biochar, and Their Amended Soil: Effects of Phosphorus Nature and Soil Property. *J. Environ. Qual* **2014**, *43* (4), 1504−1509.
(15) Gunes, A.; Inal, A.; Taskin, M. B.; Sahin, O.; Kaya, E. C.; Atakol, A. Effect of phosphorus-enriched biochar and poultry manure on growth and mineral composition of lettuce (Lactuca sativa L. cv.) grown in alkaline soil. *Soil Use Manage.* **2014**, *30* (2), 182−188.
(16) Funke, A.; Ziegler, F. Hydrothermal carbonization of biomass: A summary and discussion of chemical mechanisms for process engineering. *Biofuels, Bioprod. Biorefin.* **2010**, *4* (2), 160−177.
(17) Mohan, D.; Pittman, C. U.; Steele, P. H. Pyrolysis of wood/biomass for bio-oil: a critical review. *Energy Fuels* **2006**, *20* (3), 848−889.
(18) Cao, X.; Ro, K. S.; Chappell, M.; Li, Y.; Mao, J. Chemical Structures of Swine-Manure Chars Produced under Different Carbonization Conditions Investigated by Advanced Solid-State 13C Nuclear Magnetic Resonance (NMR) Spectroscopy. *Energy Fuels* **2011**, *25* (1), 388−397.
(19) Xu, Y. L.; Chen, B. L. Investigation of thermodynamic parameters in the pyrolysis conversion of biomass and manure to biochars using thermogravimetric analysis. *Bioresour. Technol.* **2013**, *146*, 485−493.
(20) Cantrell, K. B.; Hunt, P. G.; Uchimiya, M.; Novak, J. M.; Ro, K. S. Impact of pyrolysis temperature and manure source on physicochemical characteristics of biochar. *Bioresour. Technol.* **2012**, *107*, 419−428.
(21) Pagliari, P. H.; Laboski, C. A. M. Investigation of the Inorganic and Organic Phosphorus Forms in Animal Manure. *J. Environ. Qual* **2012**, *41* (3), 901−910.
(22) Novak, J. M.; Spokas, K. A.; Cantrell, K. B.; Ro, K. S.; Watts, D. W.; Glaz, B.; Busscher, W. J.; Hunt, P. G. Effects of biochars and hydrochars produced from lignocellulosic and animal manure on fertility of a Mollisol and Entisol. *Soil Use Manage.* **2014**, *30* (2), 175−181.
(23) Ma, Y. L.; Matsunaka, T. Biochar derived from dairy cattle carcasses as an alternative source of phosphorus and amendment for soil acidity. *Soil Sci. Plant Nutr.* **2013**, *59* (4), 628−641.
(24) Revell, K. T.; Maguire, R. O.; Agblevor, F. A. Influence of Poultry Litter Biochar on Soil Properties and Plant Growth. *Soil Sci.* **2012**, *177* (6), 402−408.
(25) Xu, G.; Zhang, Y.; Shao, H.; Sun, J. Pyrolysis temperature affects phosphorus transformation in biochar: Chemical fractionation and 31P NMR analysis. *Sci. Total Environ.* **2016**, *569−570*, 65−72.
(26) Uchimiya, M.; Hiradate, S.; Antal, M. J. Dissolved Phosphorus Speciation of Flash Carbonization, Slow Pyrolysis, and Fast Pyrolysis Biochars. *ACS Sustainable Chem. Eng.* **2015**, *3* (7), 1642−1649.
(27) Uchimiya, M.; Hiradate, S. Pyrolysis Temperature-Dependent Changes in Dissolved Phosphorus Speciation of Plant and Manure Biochars. *J. Agric. Food Chem.* **2014**, *62* (8), 1802−1809.
(28) Heilmann, S. M.; Molde, J. S.; Timler, J. G.; Wood, B. M.; Mikula, A. L.; Vozhdayev, G. V.; Colosky, E. C.; Spokas, K. A.; Valentas, K. J. Phosphorus Reclamation through Hydrothermal Carbonization of Animal Manures. *Environ. Sci. Technol.* **2014**, *48* (17), 10323−10329.
(29) Ekpo, U.; Ross, A. B.; Camargo-Valero, M. A.; Fletcher, L. A. Influence of pH on hydrothermal treatment of swine manure: Impact on extraction of nitrogen and phosphorus in process water. *Bioresour. Technol.* **2016**, *214*, 637−644.
(30) Dai, L. C.; Tan, F. R.; Wu, B.; He, M. X.; Wang, W. G.; Tang, X. Y.; Hu, Q. C.; Zhang, M. Immobilization of phosphorus in cow manure during hydrothermal carbonization. *J. Environ. Manage.* **2015**, *157*, 49−53.
(31) Wang, T.; Zhai, Y.; Zhu, Y.; Peng, C.; Wang, T.; Xu, B.; Li, C.; Zeng, G. Feedwater pH affects phosphorus transformation during hydrothermal carbonization of sewage sludge. *Bioresour. Technol.* **2017**, *245*, 182−187.
(32) Huang, R.; Tang, Y. Speciation Dynamics of Phosphorus during (Hydro)Thermal Treatments of Sewage Sludge. *Environ. Sci. Technol.* **2015**, *49* (24), 14466−14474.
(33) Huang, R.; Tang, Y. Evolution of phosphorus complexation and mineralogy during (hydro)thermal treatments of activated and anaerobically digested sludge: Insights from sequential extraction and P K-edge XANES. *Water Res.* **2016**, *100*, 439−447.
(34) Huang, R.; Fang, C.; Lu, X.; Jiang, R.; Tang, Y. Transformation of Phosphorus during (Hydro)thermal Treatments of Solid Biowastes: Reaction Mechanisms and Implications for P Reclamation and Recycling. *Environ. Sci. Technol.* **2017**, *51* (18), 10284−10298.
(35) Hedley, M. J.; Stewart, J. W. B.; Chauhan, B. S. Changes in Inorganic and Organic Soil Phosphorus Fractions Induced by Cultivation Practices and by Laboratory Incubations. *Soil Sci. Soc. Am. J.* **1982**, *46* (5), 970−976.
(36) APHA. *Standard Methods for the Examination of Water and Wastewater*, 22nd ed.; American Public Health Association/American Water Works Association/Water Environment Federation: Washington DC, 2012.
(37) Murphy, J.; Riley, J. P. A modified single solution method for the determination of phosphate in natural waters. *Anal. Chim. Acta* **1962**, *27*, 31−36.
(38) do Nascimento, C. A. C.; Pagliari, P. H.; Schmitt, D.; He, Z.; Waldrip, H. Phosphorus Concentrations in Sequentially Fractionated Soil Samples as Affected by Digestion Methods. *Sci. Rep.* **2016**, *5*, 17967.
(39) Ravel, á.; Newville, M. ATHENA, ARTEMIS, HEPHAESTUS: data analysis for X-ray absorption spectroscopy using IFEFFIT. *J. Synchrotron Radiat.* **2005**, *12* (4), 537−541.
(40) Laurencin, D.; Almora-Barrios, N.; de Leeuw, N. H.; Gervais, C.; Bonhomme, C.; Mauri, F.; Chrzanowski, W.; Knowles, J. C.; Newport, R. J.; Wong, A.; Gan, Z.; Smith, M. E. Magnesium incorporation into hydroxyapatite. *Biomaterials* **2011**, *32* (7), 1826−1837.
(41) Cao, X.; Harris, W. Carbonate and Magnesium Interactive Effect on Calcium Phosphate Precipitation. *Environ. Sci. Technol.* **2008**, *42* (2), 436−442.
(42) Lott, J. N. A.; Ockenden, I.; Raboy, V.; Batten, G. D. Phytic acid and phosphorus in crop seeds and fruits: a global estimate. *Seed Sci. Res.* **2000**, *10* (1), 11−33.
(43) Toor, G. S.; Cade-Menun, B. J.; Sims, J. T. Establishing a linkage between phosphorus forms in dairy diets, feces, and manures. *J. Environ. Qual.* **2005**, *34* (4), 1380−1391.
(44) Toor, G. S.; Peak, J. D.; Sims, J. T. Phosphorus speciation in broiler litter and turkey manure produced from modiried diets. *J. Environ. Qual.* **2005**, *34* (2), 687−697.
(45) Leytem, A. B.; Plumstead, P. W.; Maguire, R. O.; Kwanyuen, P.; Brake, J. What aspect of dietary modification in broilers controls litter water-soluble phosphorus: Dietary phosphorus, phytase, or calcium? *J. Environ. Qual.* **2007**, *36* (2), 453−463.
(46) Azuara, M.; Kersten, S. R. A.; Kootstra, A. M. J. Recycling phosphorus by fast pyrolysis of pig manure: Concentration and extraction of phosphorus combined with formation of value-added pyrolysis products. *Biomass Bioenergy* **2013**, *49*, 171−180.
(47) Liu, W. J.; Zeng, F. X.; Jiang, H.; Yu, H. Q. Total recovery of nitrogen and phosphorus from three wetland plants by fast pyrolysis technology. *Bioresour. Technol.* **2011**, *102* (3), 3471−3479.
(48) Christensen, P. S.; Peng, G. l.; Vogel, F.; Iversen, B. B. Hydrothermal liquefaction of the microalgae Phaeodactylum tricornutum: impact of reaction conditions on product and elemental distribution. *Energy Fuels* **2014**, *28* (9), 5792−5803.
(49) Pagliari, P. H.; Laboski, C. A. M. Dairy manure treatment effects on manure phosphorus fractionation and changes in soil test phosphorus. *Biol. Fertil. Soils* **2013**, *49* (8), 987−999.
(50) Pagliari, P. H., Variety and Solubility of Phosphorus Forms in Animal Manure and Their Effects on Soil Test Phosphorus. In *Applied Manure and Nutrient Chemistry for Sustainable Agriculture and*

DOI: 10.1021/acs.est.7b05203
Environ. Sci. Technol. 2018, 52, 3016−3026

Environment; He, Z., Zhang, H., Eds.; Springer Netherlands: Dordrecht, 2014; pp 141−161.
(51) Ingall, E. D.; Brandes, J. A.; Diaz, J. M.; de Jonge, M. D.; Paterson, D.; McNulty, I.; Elliott, W. C.; Northrup, P. Phosphorus K-edge XANES spectroscopy of mineral standards. *J. Synchrotron Radiat.* **2011**, *18*, 189−197.
(52) Brandes, J. A.; Ingall, E.; Paterson, D. Characterization of minerals and organic phosphorus species in marine sediments using soft X-ray fluorescence spectromicroscopy. *Mar. Chem.* **2007**, *103* (3−4), 250−265.
(53) He, Z.; Pagliari, P. H.; Waldrip, H. M. Applied and Environmental Chemistry of Animal Manure: A Review. *Pedosphere* **2016**, *26* (6), 779−816.
(54) Werner, F.; Prietzel, J. Standard Protocol and Quality Assessment of Soil Phosphorus Speciation by P K-Edge XANES Spectroscopy. *Environ. Sci. Technol.* **2015**, *49* (17), 10521−10528.
(55) Libra, J. A.; Ro, K. S.; Kammann, C.; Funke, A.; Berge, N. D.; Neubauer, Y.; Titirici, M.-M.; Fühner, C.; Bens, O.; Kern, J.; Emmerich, K.-H. Hydrothermal carbonization of biomass residuals: a comparative review of the chemistry, processes and applications of wet and dry pyrolysis. *Biofuels* **2011**, *2* (1), 71−106.
(56) Bruun, S.; Harmer, S.; Bekiaris, G.; Christel, W.; Zuin, L.; Hu, Y.; Jensen, L. S.; Lombi, E. The effect of different pyrolysis temperatures on the speciation and availability in soil of P in biochar produced from the solid fraction of manure. *Chemosphere* **2017**, *169*, 377−386.
(57) Zwetsloot, M. J.; Lehmann, J.; Solomon, D. Recycling slaughterhouse waste into fertilizer: how do pyrolysis temperature and biomass additions affect phosphorus availability and chemistry? *J. Sci. Food Agric.* **2015**, *95* (2), 281−288.
(58) Li, R.; Zhang, Z.; Li, Y.; Teng, W.; Wang, W.; Yang, T. Transformation of apatite phosphorus and non-apatite inorganic phosphorus during incineration of sewage sludge. *Chemosphere* **2015**, *141*, 57−61.
(59) Kasioptas, A.; Geisler, T.; Perdikouri, C.; Trepmann, C.; Gussone, N.; Putnis, A. Polycrystalline apatite synthesized by hydrothermal replacement of calcium carbonates. *Geochim. Cosmochim. Acta* **2011**, *75* (12), 3486−3500.
(60) Liu, J.; Ye, X.; Wang, H.; Zhu, M.; Wang, B.; Yan, H. The influence of pH and temperature on the morphology of hydroxyapatite synthesized by hydrothermal method. *Ceram. Int.* **2003**, *29* (6), 629−633.

DOI: 10.1021/acs.est.7b05203
Environ. Sci. Technol. 2018, 52, 3016−3026